AIAA-90-0124

A CRITERIA FOR SURFACE PRESSURE SPECIFICATION IN AERODYNAMIC SHAPE DESIGN

G. S. Dulikravich
Penn State University
University Park, PA 16802

28th Aerospace Sciences Meeting
January 8-11, 1990/Reno, Nevada

A CRITERIA FOR SURFACE PRESSURE SPECIFICATION IN AERODYNAMIC SHAPE DESIGN

George S. Dulikravich*

Department of Aerospace Engineering
The Pennsylvania State University
University Park, PA 16802 USA

ABSTRACT

A conceptually new analytic criteria for detection of fluid flow separation in general multidimensional, steady and unsteady, compressible and incompressible flow situations has been introduced, verified and generalized. The new formulation offers new possibilities for the inverse design of aerodynamic shapes when flow separatin should be prevented over a range of operating conditions. Specifically, the generalized analytic formulation can be easily used to check the reliability of any specified surface pressure variation. Furthermore, it can be used for the derivation of analytic expressions for families of acceptable surface pressure variations to be used in inverse design of aerodynamic configurations.

INTRODUCTION

Methodologies for determining appropriate shapes of aerodynamic objects can be separated in two distinct groups. The first group involves methods for the flow field inverse design where certain criterions are to be satisfied in the flow field. An example is the shock-free flow field design using fictitious gas formulation [1,2] where the aerodynamic shape will guarantee an entirely shock-free flow field, but will not enable us to prescribe surface velocity distribution.

The second group of methods belongs to surface inverse design where certain criteria are to be satisfied on the surface of the object irregardless of the possible consequences in the flow field. An example is the method developed by Volpe [3,4] which allows specification of quite arbitrary velocity variation along the surface of the object. At transonic speeds, although the prescribed surface velocity variation is, say, shock-free, a "loose-foot" or "hanging" shock may appear in the flow field above the concave part of the surface underneath the supersonic bubble.

Most of the research in aerodynamic shape inverse design and optimization has been devoted to the development of new techniques for deducing a shape of the object, assuming that the specified velocity distribution along the surface is correct. The problem of determining the best velocity distribution has not been resolved yet, though Ives [5] offers a number of useful suggestions.

The main problem facing any new aerodynamic design is flow separation, which can in reality drastically reduce the high expectations based on a specified surface velocity distribution [6].

---

* Associate Professor. Senior member AIAA.

A number of analytic criteria have been developed for enabling a designer to specify a more reliable velocity distribution. Probably the best review of the existing criteria for two-dimensional, incompressible, steady, laminar separation is contained in an excellent paper by Zhang [7]. He also offers a new analytic separation criterion for such flows.

Nevertheless, for three-dimensional flows, and for compressible flows, there are no known universal criteria for flow separation that can be easily utilized when prescribing the desired surface velocity distribution. Development of such new universal flow separation criteria for general three-dimensional, compressible, unsteady flows is the objective of this work.

MINIMUM KINETIC ENERGY RATE CRITERION

A conceptually entirely new approach to flow separation was suggested by Sih [8] in his enlightening description of the phenomenological link between fracture mechanics and flow separation. He suggested that in the case of a thin viscous boundary layer "the inviscid flow around a solid body coupled with a criteria of separation may provide sufficient information to forecast separation." Consequently, Sih [8] postulates that "separation occurs at the location near the boundary where the rate of increase of potential energy density is a local maximum," concluding that "it is easier to search for minima in the rate of decrease of kinetic energy density" than to find the maxima of the increase of the potential energy. He then proceeds by demonstrating this principle on two examples: a steady, incompressible, irrotational flow around a circular cylinder and a flow around an elliptic cylinder at different angles of attack. The predicted locations of separation points using his criteria are in a reasonable agreement with experimental data.

In order to verify this concept, several published experimental data for measured surface pressure distributions over different shapes have been analyzed by computing and plotting the kinetic energy rate variation along the surface. The results were quite convincing. Figures 1-3 demonstrate that general flow separation criteria is valid over a range of Reynolds numbers for a steady incompressible flow over circular cylinder [9,10,11]. Figures 4-6 reconfirm the reliability of the method by applying it to flows over an elliptic non-lifting cylinder at different Reynolds numbers [11]. The concept also gives reliable prediction (Figs. 7-8) of separation points for high Reynolds numbers and NACA 663-018 airfoil shape [12]. It was interesting to see that Sih's concept works remarkably at transonic speeds as well. Careful numerical results obtained by Olling and Dulikravich [13] for a transonic, steady, shocked flow around a RAE 2822 airfoil [14] shows the experimental surface velocity (Figure 9) distribution and shows the corresponding variation of

the kinetic energy rate (Figure 10). Sih's concept clearly detects post-shock separation and a tendency toward leading edge separation as it was confirmed by numerical experiments [13].

Finally, the new concept was tested against three-dimensional experimental results for a very low Reynolds number incompressible flow over a rectangular wing at different angles of attack [15,16]. The experimental results at different angles of attack are summarized in Figures 11 and 12 where S and R designate separation and reattachment points, respectively. A more complete summary of experimentally observed locations of S and R points is presented in [15,16]. The corresponding plots of quasi-twodimensional variation of the kinetic energy rate are shown in Figures 13-14 demonstrating the validity of Sih's concept for detection of separation points. The following general analytic formulation is valid for multi-dimensional, steady and unsteady, compressible and incompressible flow separation detection based on a minimum variation of the kinetic energy rate.

THEORETICAL FORMULATION

The sum of kinetic energy, T, and potential energy, U, is a constant at any instant of time

$$\frac{D(T+U)}{Dt} = \dot{T} + \dot{U} = 0 \tag{1}$$

Local instantaneous value of the kinetic energy is

$$T = \frac{1}{2}\rho q^2 \quad . \tag{2}$$

where ρ is the local fluid density, and the local velocity vector is defined as

$$\vec{q} = q\hat{e}_s + 0\hat{e}_n + 0\hat{e}_m \tag{3}$$

Here, (s,n,m) form a locally streamline aligned Cartesian coordinate system. Then, total time rate of change of the kinetic energy is

$$\dot{T} = \frac{DT}{Dt} = \frac{\partial T}{\partial t} + (\vec{q}\cdot\nabla)T = \frac{\partial}{\partial t}(\frac{1}{2}\rho q^2) + q\frac{\partial T}{\partial s} \tag{4}$$

This can be rewritten as

$$\dot{T} = \frac{1}{2}q^2\rho_t + \rho q q_t + \frac{1}{2}q^3\rho_s + \rho q^2 q_s \tag{5}$$

In the case of an isentropic fluid flow, normalized density is given as

$$\rho = \frac{\bar{\rho}}{\bar{\rho}_o} = [\frac{\gamma+1}{2} - \frac{\gamma-1}{2}q^2]^{\frac{1}{\gamma-1}} \tag{6}$$

where an over-bar designates dimensional quantities and critical Mach number is defined as

$$q = \frac{\bar{q}}{\bar{a}_o} = M_o \tag{7}$$

Then, the time rate of change of kinetic energy is

$$\dot{T} = \frac{1}{2}q^2(\frac{1}{\gamma-1})[\frac{\gamma+1}{2} - \frac{\gamma-1}{2}q^2]^{\frac{1}{\gamma-1}-1}(-\frac{\gamma-1}{2})2qq_t + \rho q q_t + \rho q^2 q_s - \frac{1}{2}q^3[\frac{\gamma+1}{2} - \frac{\gamma-1}{2}q^2]^{\frac{1}{\gamma-1}} - 1(\frac{1}{\gamma-1})(\frac{\gamma-1}{2}2qq_s) \tag{8}$$

Note also that the local isentropic speed of sound is defined as

$$a^2 = \frac{\bar{a}^2}{\bar{a}_o^2} = [\frac{\gamma+1}{2} - \frac{\gamma-1}{2}q^2] \tag{9}$$

Then

$$\dot{T} = -\frac{1}{2}\rho\frac{q^2}{a^2}qq_t + \rho q q_t + \rho q^2 q_s - \frac{1}{2}\rho\frac{q^2}{a^2}q^2 q_s \tag{10}$$

Since the local Mach number is by definition

$$M = \frac{q}{a} \tag{11}$$

it follows that

the time rate of change of the kinetic energy is

$$\dot{T} = (1 - \frac{M^2}{2})\rho q(q_t + q q_s) \tag{12}$$

Our objective is to find the minimas of the time rate of change of the local kinetic energy, that is, to find the locations of points where

$$\dot{T} = \frac{D\dot{T}}{Dt} = 0 \tag{13}$$

The streamwise gradient of the rate of change of the local kinetic energy is

$$\frac{\partial\dot{T}}{\partial s} = \dot{T}_s = (1 - \frac{M^2}{2})_s \rho q(q_t + q q_s) + (1 - \frac{M^2}{2})\rho_s q(q_t + q q_s) + (1 - \frac{M^2}{2})\rho q_s(q_t + q q_s) + (1 - \frac{M^2}{2})\rho q(q_{ts} + (q_s)^2 + q q_{ss}) \tag{14}$$

Since

$$M^2 = \frac{q^2}{a^2} = \frac{q^2}{\frac{\gamma+1}{2} - \frac{\gamma-1}{2}q^2} \quad , \tag{15}$$

it follows that

$$(M^2)_s = [2\frac{q}{a^2} + (\gamma-1)M^2\frac{q}{a^2}]q_s \quad . \tag{16}$$

Also, note that

$$\rho_s = -\frac{\rho}{a^2}qq_s \quad . \tag{17}$$

Furthermore,

$$\ddot{T} = \frac{D\dot{T}}{Dt} = \frac{\partial\dot{T}}{\partial t} + (\vec{q}\cdot\nabla)\dot{T} \ , \tag{18}$$

where

$$\frac{\partial\dot{T}}{\partial t} = (1 - \frac{M^2}{2})_t \rho q(q_t + q q_s) + (1 - \frac{M^2}{2})\rho_t q(q_t + q q_s) + (1 - \frac{M^2}{2})\rho q_t(q_t + q q_s) + (1 - \frac{M^2}{2})\rho q(q_{tt} + q_t q_s + q q_{st}) \tag{19}$$

and

$$(\vec{q}\cdot\nabla)\dot{T} = q\dot{T}_s = q(1 - \frac{M^2}{2})_s \rho q(q_t + q q_s) + q(1 - \frac{M^2}{2})\rho_s q(q_t + q q_s) + q(1 - \frac{M^2}{2})\rho q_s(q_t + q q_s) + q(1 - \frac{M^2}{2})\rho q(q_{ts} + (q_s)^2 + q q_{ss}) \tag{20}$$

Hence, the time rate of change of the time rate of change of the local kinetic energy is

$$\dot{T} = -\frac{1}{2}\frac{2qq_t a^2 - q^2(-\frac{\gamma-1}{2})2qq_t}{(a^2)^2}\rho q(q_t + qq_s)$$
$$+ (1 - \frac{M^2}{2})\frac{1}{\gamma-1}[\frac{\gamma+1}{2} - \frac{\gamma-1}{2}q^2]^{\frac{1}{\gamma-1}-1}$$
$$(-\frac{\gamma-1}{2}2qq_t)q(q_t+qq_s) + (1 - \frac{M^2}{2})\rho[(q_t)^2 + qq_tq_s$$
$$+ qq_{tt} + qq_tq_s + q^2q_{st}] - (M^2 + \frac{\gamma-1}{2}M^4)q_s\rho q(q_t + qq_s)$$
$$- (1 - \frac{M^2}{2})M^2q\rho q_s(q_t + qq_s) + (1 - \frac{M^2}{2})\rho q[q_sq_t + q(q_s)^2$$
$$+ qq_{ts} + q(q_s)^2 + q^2q_{ss}] . \quad (21)$$

Finally, the locations of separation points should be determined from the condition that

$$\dot{T} = \rho\{[1 - \frac{5}{2}M^2 + \frac{2-\gamma}{2}M^4](q_t + qq_s)^2 + (1 - \frac{M^2}{2})$$
$$[qq_sq_t + 2q^2q_{st} + qq_{tt} + q^2(q_s)^2 + q^3q_{ss}]\} = 0 \quad (22)$$

In the case of a steady flow of an incompressible fluid, this condition reduces to

$$\dot{T} = \rho q^2(q_s)^2 + q^3q_{ss} = \rho[q(q^2q_s)_s] = 0. \quad (23)$$

In the case of an unsteady incompressible flow, the general flow separation condition reduces to

$$\dot{T} = \rho\{(q_t + qq_s)^2 + [q_sq_t + 2qq_{st} + q_{tt} + q(q_s)^2$$
$$+ q^2q_{ss}]q\} = 0 \quad (24)$$

In the case of a steady compressible flow, the general flow separation condition becomes

$$\dot{T} = \rho q^2\{[2 - 3M^2 + \frac{2-\gamma}{2}M^4](q_s)^2 + qq_{ss}(1 - \frac{M^2}{2})\} = 0 \quad (25)$$

EXAMPLE

Let us consider a two-dimensional steady potential flow of an incompressible inviscid fluid past a stationary circular cylinder of radius r_o. The radial component of the local velocity vector is given as

$$u^r = q_\infty(1 - \frac{r_o^2}{r^2})\cos\theta \quad (26)$$

and the tangential component of velocity is given as

$$u^\theta = -q_\infty(1 + \frac{r_o^2}{r^2})\sin\theta \quad (27)$$

Then

$$q^2 = q_\infty^2[1 + (\frac{r_o}{r})^4 - \frac{2r_o^2\cos 2\theta}{r^2}] \quad (28)$$

and (from Eq. 23)

$$\dot{T} = \rho q^2[2(q_s)^2 + qq_{ss}] = \rho q^2[2(q_\theta)^2 + qq_{\theta\theta}] = 0 \quad (29)$$

on the surface of the cylinder. There, we also have that $r = r_o$. Then

$$q^2 = q_\infty^2[2 - 2\cos 2\theta] \quad (30)$$

and

$$q_\theta = q_\infty\frac{2\sin 2\theta}{\sqrt{2 - 2\cos 2\theta}} \quad (31)$$

and

$$q_{\theta\theta} = q_\infty\frac{4\cos 2\theta\sqrt{2 - 2\cos 2\theta} - \sin 2\theta\left(\frac{4\sin 2\theta}{\sqrt{2-2\cos 2\theta}}\right)}{2 - 2\cos 2\theta} \quad (32)$$

Hence,

$$\dot{T} = 2q_\infty^2\frac{4\sin^2 2\theta}{2 - 2\cos 2\theta}$$
$$+ q_\infty^2\frac{4\cos 2\theta(2 - 2\cos 2\theta) - 4\sin^2 2\theta}{2 - 2\cos 2\theta} = 0 \quad (33)$$

Since $\sin^2 2\theta = 1 - \cos^2 2\theta$, it follows that the following equation must be satisfied at the separation points determined from

$$-12\cos^2 2\theta + 8\cos 2\theta + 4 = 0 . \quad (34)$$

This means that the location of separation points is at

$$\cos 2\theta = -\frac{1}{3} \therefore \theta = \pm 54.73^\circ \quad (35)$$

and that the stagnation points are located at

$$\cos 2\theta = 1 \therefore \theta = 0, \pm\pi \quad (36)$$

Experimentally observed location of separation points at high Reynolds number flows ($Re > 10^6$) is between $\theta_{sep} = 52^\circ$ and $\theta_{sep} = 58^\circ$ measured from the trailing edge of the circle.

Since potential flow theory is valid outside the boundary layer and since the thickness of the boundary layer decreases with the increase in Reynolds number, one should expect even better agreement between this theory and experiments for higher Reynolds numbers.

ACKNOWLEDGMENTS

The author is thankful to his assistants, Mr. T.-L. Chiang, R. Kampia and B. Kosovic for their help with graphics. Thanks to Ms. Amy Myers for her excellent typing.

REFERENCES

1. Sobieczky, H., "Transonic Fluid Dynamics-Lecture Notes," University of Arizona, TFD, 77-01, October 1977.

2. Dulikravich, G. S. and Sobieczky, H., "Shockless Design and Analysis of Transonic Cascade Shapes," AIAA Journal, Vol. 20, No. 11, Nov. 1982, pp. 1572-1578.

3. Volpe, G. and Melnik,. R. E., "The Design of Transonic Airfoils by a Well-Posed Inverse Method," Proceedings of the First Int. Conf. on Inverse Design Concepts in Engineering Sciences (ICIDES-I), editor: G. S. Dulikravich, The Univ. of Texas at Austin, Oct. 17-18, 1984.

4. Volpe, G., "On the Design of Airfoil Profiles for Supercritical Pressure Distributions," Proceedings of the Second Int. Conf. on Inverse Design and

Optimization in Eng. Sciences (ICIDES-II), editor: G. S. Dulikravich, The Pennsylvania State Univ., University Park, PA., Oct. 27-28, 1987, pp. 487-506.

5. Ives, D. C., "Inverse and Hybrid Compressor Cascade Design Methods," Proceedings of the First Int. Conf. on Inverse Design Concepts in Eng. Sci., (ICIDES-I), editor: G. S. Dulikravich, The University of Texas at Austin, Oct. 17-18, 1984.

6. Liebeck, R. H., "A Class of Airfoils Designed for High Lift in Incompressible Flow," Paper No. 73-86, AIAA 11th Aerospace Sciences Meeting, Washington, D.C. 1973.

7. Zhang, H. X., "A Universal Criterion for Two Dimensional Flow Separation," The Chinese Aerodynamic Research and Development Center Report, 1983.

8. Sih, G. C., "Phenomena of Instability: Fracture Mechanics and Flow Separation," Naval Research Reviews, Spring 1980, pp. 30-42.

9. Meier, H. V., Kreplin, H. P. and Fang, L. W., "Experimental Study of Two-and-Three-Dimensional Boundary Layer Separation," Springer-Verlag, New York, 1981.

10. Roshko, A., "Unsteady Turbulent Shear Flows," Springer-Verlag, New York, 1981.

11. Goldstein, S., "Modern Developments in Fluid Dynamics," Dover, 1965.

12. Chang, P. K., "Separation of Flow," Pergamon Press, 1970.

13. Olling, C. R. and Dulikravich, G. S., "Porous Aerofoil Analysis Using Viscous-Inviscid Coupling at Transonic Speeds," Internat. Journal for Numerical Meth. in Fluids, Vol. 7, 1987, pp. 103-129.

14. Cook, P. H., McDonald, M. A. and Firmin, M. C. P., "Airfoil RAE 2822-Pressure Distributions and Boundary Layer and Wake Measurements," AGARD Advisory Report No. 138, 1979, Paper A6.

15. Bastedo, W. G. and Mueller, T. J., "Experimental Studies of the Boundary Layer Characteristics on Low Reynolds Number Airfoils Including the Three-Dimensional and Unsteady Effects," University of Notre Dame Report, UNDAS-0239-TR-1, January 1985.

16. Bastedo, W. G. and Mueller, T. J., "The Spanwise Variation of Laminar Separation Bubbles on Finite Wings at Low Reynolds Numbers," AIAA paper No. 85-139, Aerospace Sciences Meeting, Reno, NV, Jan. 1985.

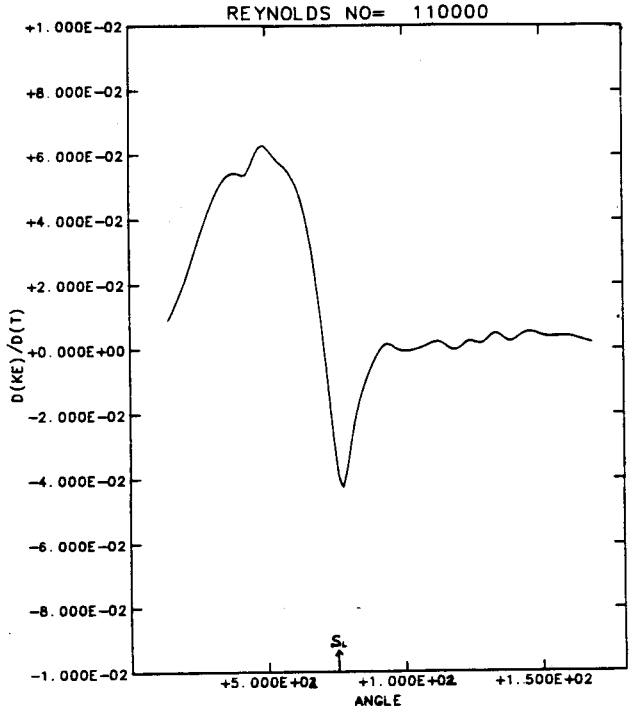

Figure 1. Circular cylinder; surface variation of the rate of change of kinetic energy; Reynolds number = 110,000; incompress.

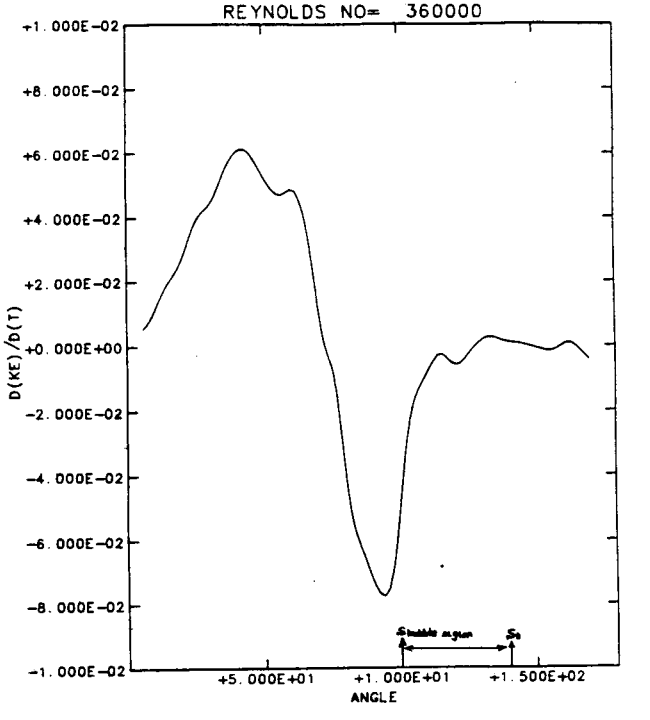

Figure 2. Circular cylinder; surface variation of the rate of change of kinetic energy; Reynolds number = 360,000; incompress.

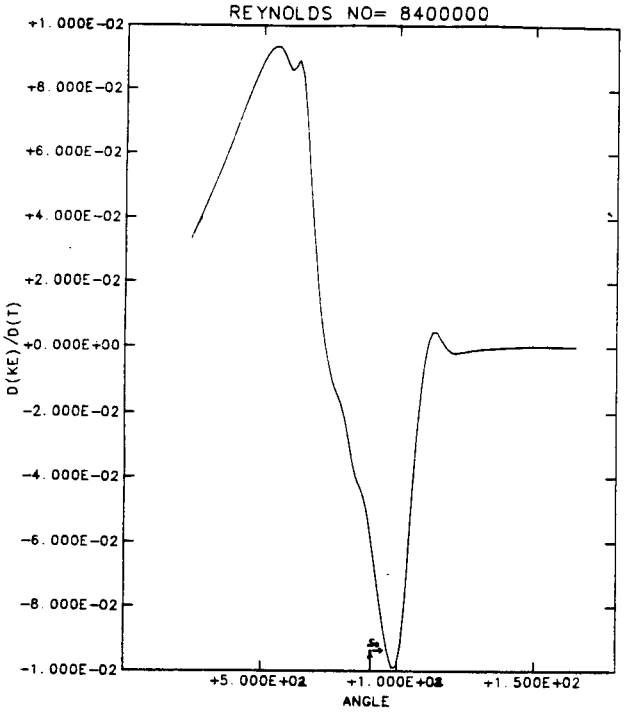

Figure 3. Circular cylinder; surface variation of the rate of change of kinetic energy; Reynolds number = 8,400,000; incompress.

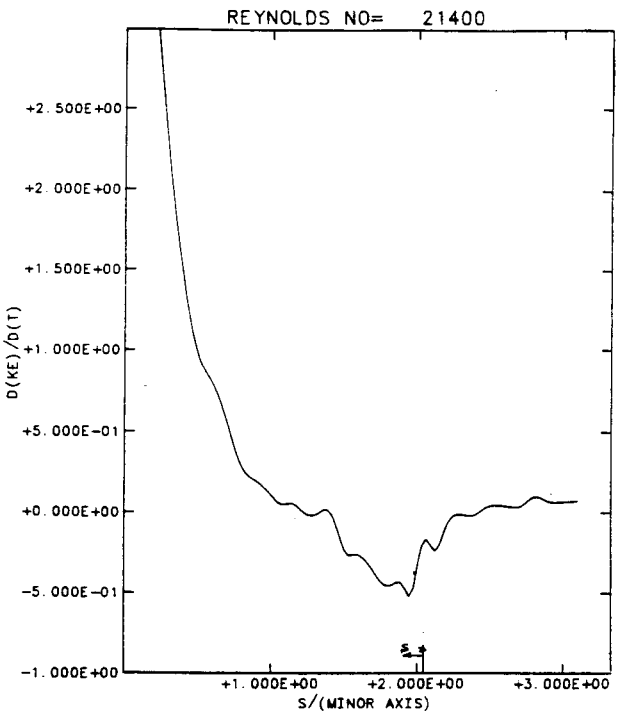

Figure 4. Elliptic cylinder; surface variation of the rate of change of kinetic energy; Reynolds number = 21,400; incompress.

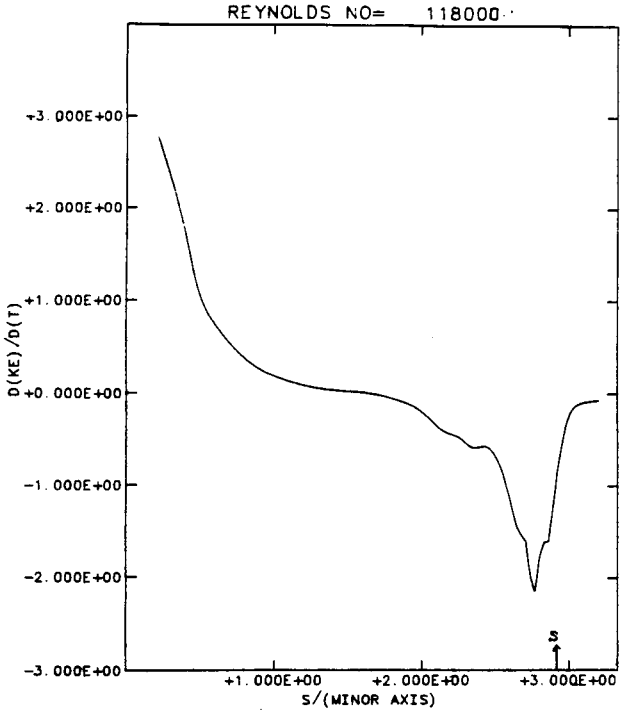

Figure 5. Elliptic cylinder; surface variation of the rate of change of kinetic energy; Reynolds number = 118,000; incompress.

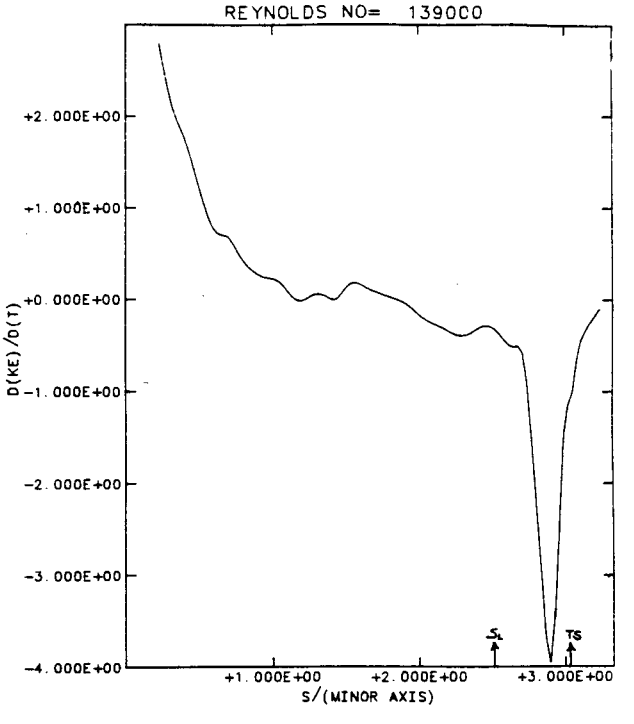

Figure 6. Elliptic cylinder; surface variation of the rate of change of kinetic energy; Reynolds number = 139,000; incompress.

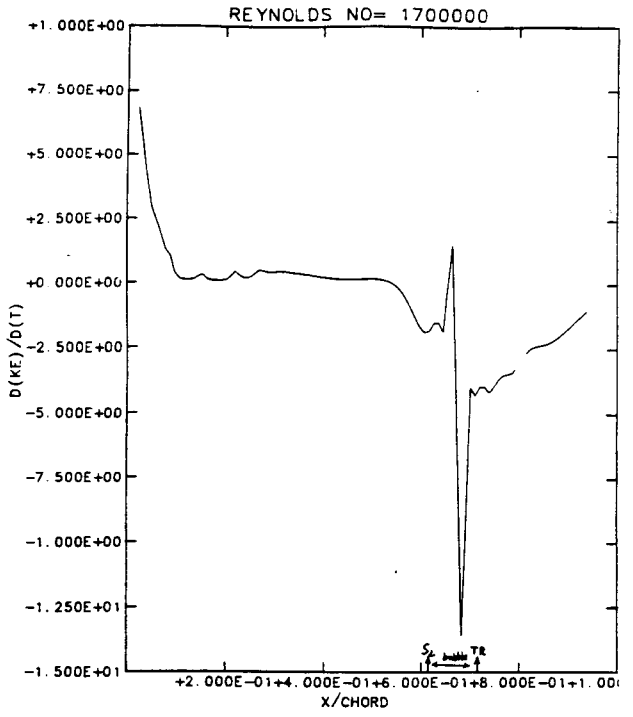

Figure 7. NACA 663-018 airfoil; surface variation of the rate of change of kinetic energy Reynolds number = 1,700,000; incompress.

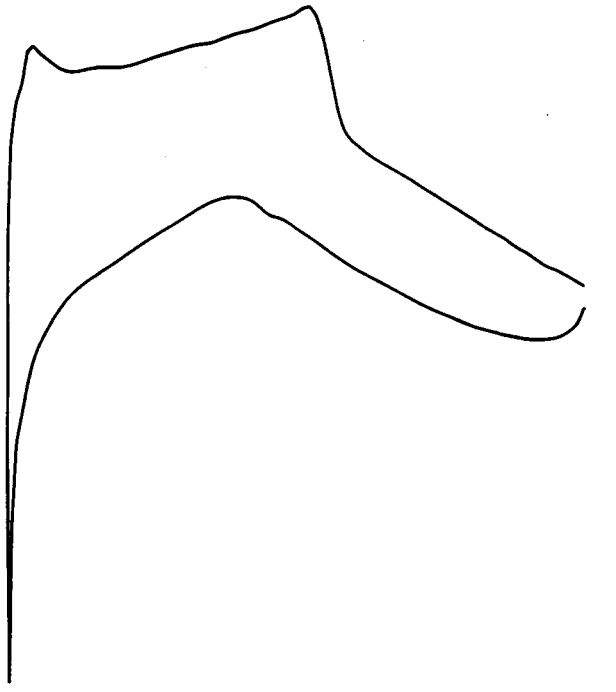

Figure 9. RAE 2822 airfoil; experimental values of surface Mach number distribution [14].

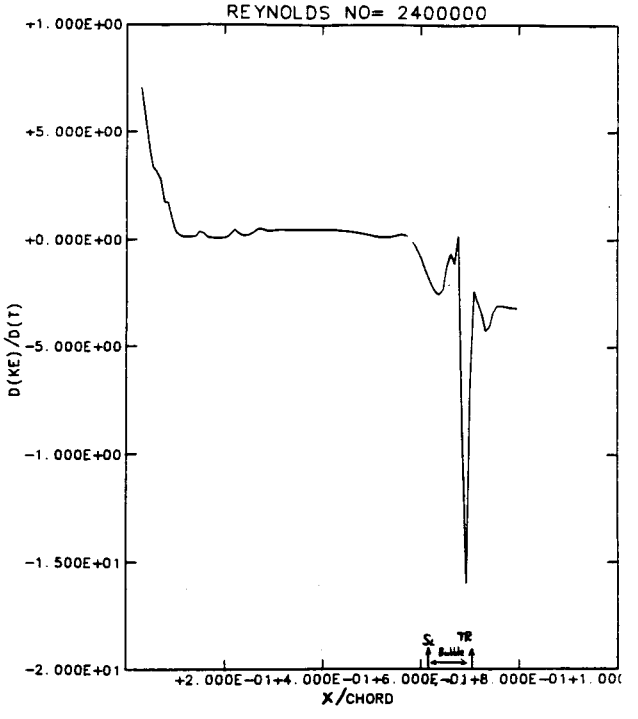

Figure 8. NACA 663-018 airfoil; surface variation of the rate of change of kinetic energy Reynolds number = 2,400,000; incompress.

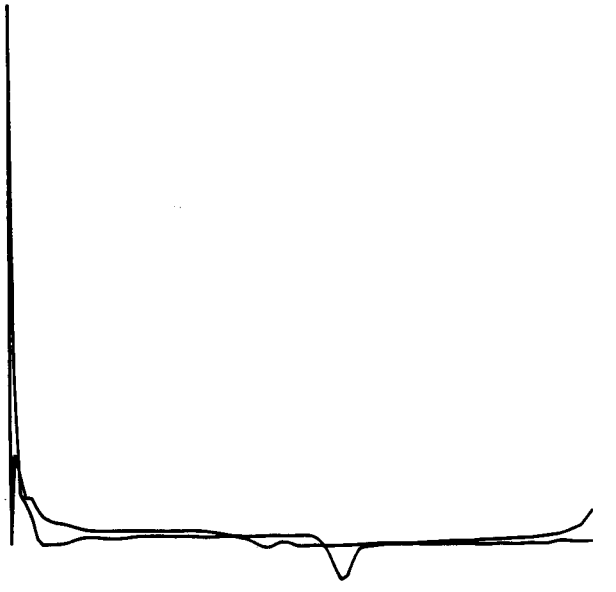

Figure 10. RAE 2822 airfoil; surface variation of the rate of change of kinetic energy; Reynolds number = 6,250,000; M_∞ = 0.723.

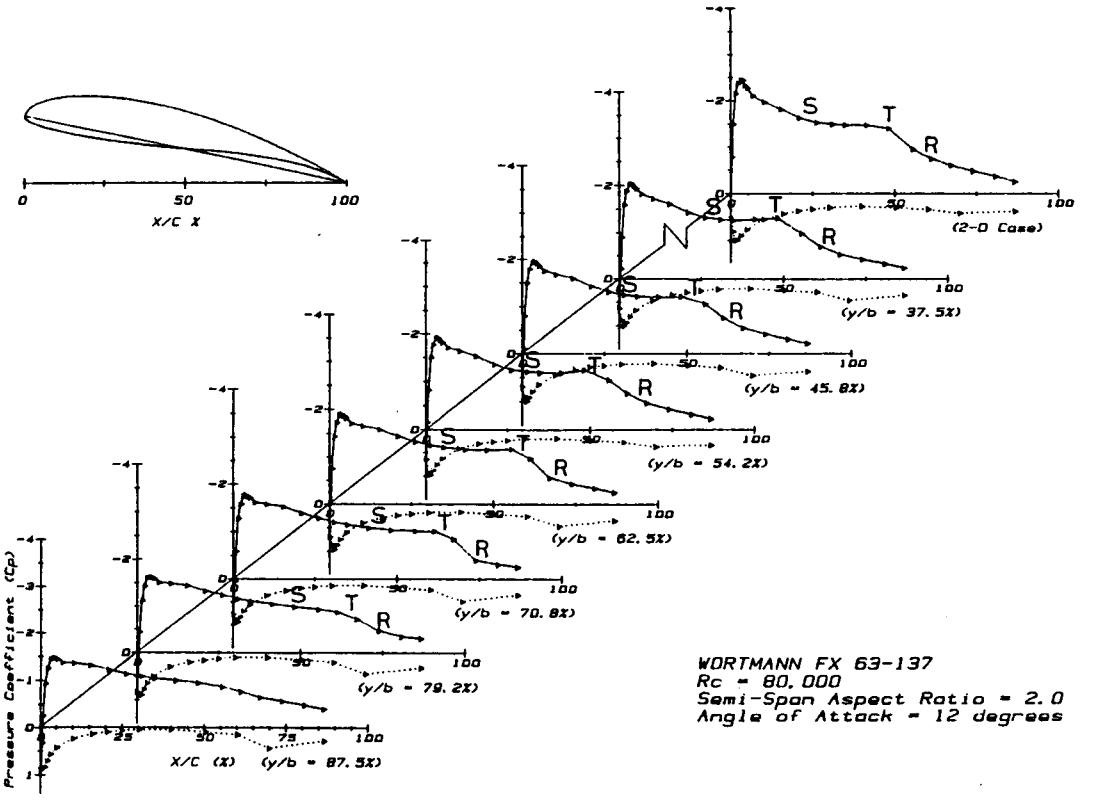

Figure 11. Rectangular wing with experimental values of sectional surface Cp distributions[15] Reynolds number = 80,000; alpha = 12°.

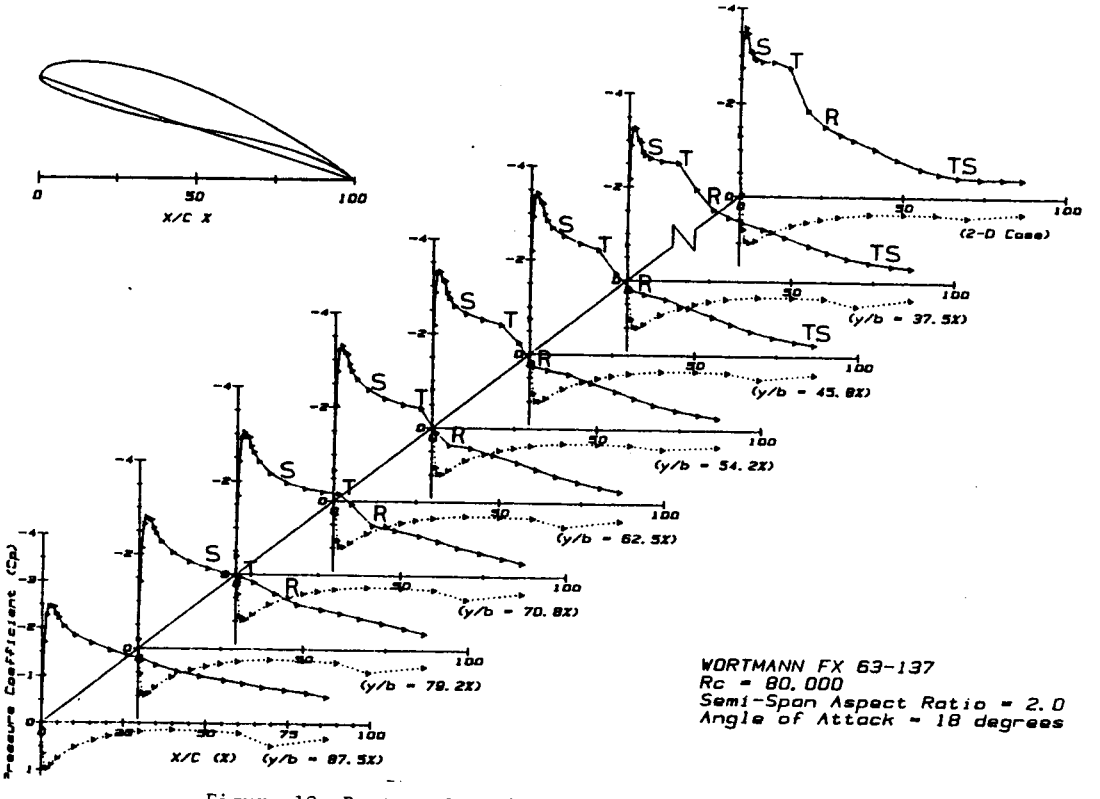

Figure 12. Rectangular wing with experimental values of sectional surface Cp distributions[16] Reynolds number = 80,000; alpha = 18°.

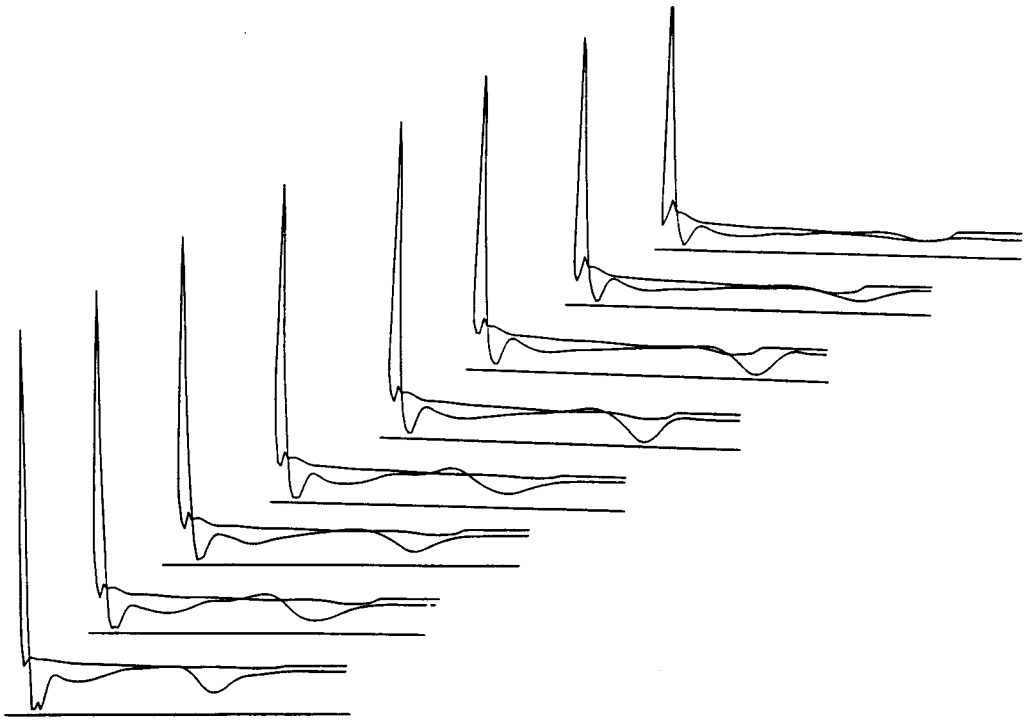

Figure 13. Rectangular wing at alpha = 12°; sectional variation of the rate of change of kinetic energy; Reynolds number = 80,000; M_∞ = 0.1.

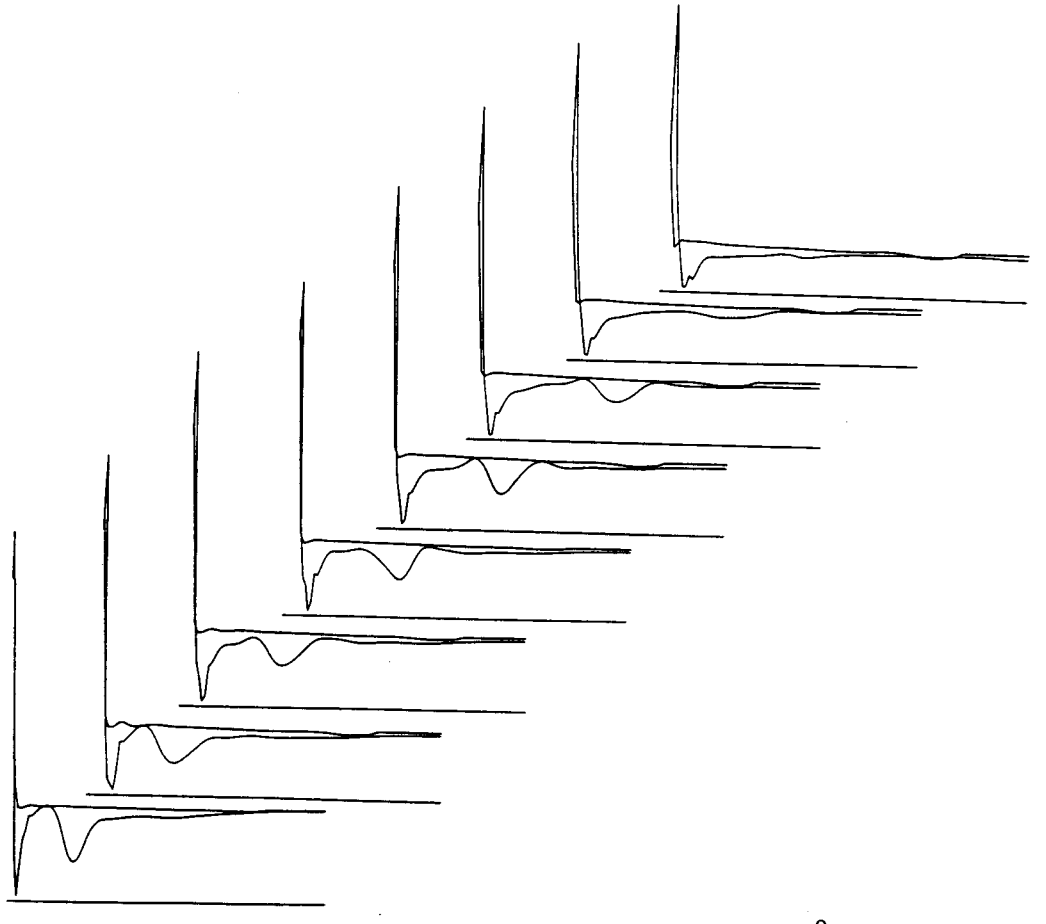

Figure 14. Rectangular wing at alpha = 18°; sectional variation of the rate of change of kinetic energy; Reynolds number = 80,000; M_∞ = 0.1.